Journal of Sustainable Construction Materials and Technologies
Web page info: https://jscmt.yildiz.edu.tr
DOI: 10.47481/jscmt.1157026

JSCMT
Journal of Sustainable Construction Materials and Technologies

Research Article

Characterization of carbon fiber reinforced conductive mortars filled with recycled ferrochrome slag aggregates

Fatih DOĞAN[1], Heydar DEHGHANPOUR[*2], Serkan SUBAŞI[3], Muhammed MARAŞLI[3]

[1]*Munzur University, Rare Earth Elements Application & Research Center, Tunceli, Türkiye*
[2]*Fibrobeton Company, R&D Center, Düzce, Türkiye*
[3]*Department of Civil Engineering, Düzce University, Engineering Faculty, Düzce, Türkiye*

ARTICLE INFO

Article history
Received: 05 August 2022
Accepted: 17 August 2022

Key words:
Carbon fiber, conductivity, dynamic resonance, ferrochrome slag aggregate, mortar

ABSTRACT

Recently, it has been known that carbon fiber, a conductive fiber, is used in different mixture designs and the development of electrically conductive cementitious materials. However, the evaluation of ferrochrome slag as a recycled aggregate in the mixture of these special concretes has still not been investigated. In this study, electrically conductive mortars were produced using 100% recycled ferrochrome slag aggregate with a particle size of less than 1 mm as filling material and using carbon fiber in 4 different ratios, 0%, 0.5%, 0.75%, and 1%. To investigate the electrical conductivity properties, the resistivity values of the samples were measured at five different times within 2–180 days. In addition, 28-day compressive strength, flexural strength, dynamic resonance, ultrasonic pulse velocity, Leeb hardness, scanning electron microscope, and X-Ray Diffraction tests were performed on all samples. The results were compared with the literature, proving that ferrochrome slag could be used as a reasonable aggregate in conductive mortars. The age effect was minimal in CF-added mixtures. With the addition of 1% CF, the resistivity values decreased approximately 40 times compared to the reference. Moreover, SEM analyses of the CF-0.75 sample showed that the CFs adhered to form a conductive network between the components in the ferrochrome-filled compact structure.

Cite this article as: Doğan, F., Dehghanpour, H., Subaşı, S., & Maraşlı, M. (2022). Characterization of carbon fiber reinforced conductive mortars filled with recycled ferrochrome slag aggregates. *J Sustain Const Mater Technol*, 7(3), 145–157.

1. INTRODUCTION

Cement and aggregate, used extensively in the construction sector, threaten the consumption of natural resources with each passing day. Therefore, different researches were carried out on industrial waste in concrete production [1]. Using industrial wastes as aggregates is important in reducing natural resource consumption and environmental impacts [2]. Industrial wastes, which are used instead of different components in concrete, improve concrete's mechanical and electrical properties. Research on alternative materials is continuing to minimize the greenhouse gases emerging from cement production, which is the main component material of concrete, and reduce en-

***Corresponding author.**
*E-mail address: heydar.dehghanpour@fibrobeton.com.tr

ergy consumption. In addition, since the aggregates used in concrete production cause the consumption of natural resources, alternative material studies are carried out [3]. Since concrete, used as a basic material in structures such as buildings and bridges, exhibits brittle behavior under high pressure, various research has been carried out to improve the mechanical properties of concrete [4, 5]. Aggregate, which constitutes the largest volume of the composition in the concrete mix, plays a decisive role in terms of concrete strength and workability. Studies use industrial waste products such as copper, steel, and ferrochrome wastes instead of aggregates in the cement mixture [2]. Ferrochrome waste is one of the wastes preferred instead of aggregate in concrete production related to the reuse of industrial wastes [6]. Considering its adhesion and mechanical properties, it is seen as an alternative component that can be used instead of the aggregate used in the concrete mix [7]. It has been reported that ferrochrome waste particles have a higher density than aggregates [8]. If the ferrochrome waste released because of global ferrochrome production could be taken under control and reused, natural resources would be used more efficiently. In this context, it is foreseen that the use of ferrochrome waste in cement production will be beneficial in terms of both cost reduction and energy savings. In the study of Niemela and Kauppi [9], it was reported that ferrochrome waste is chemically stable and can be used safely. Also, Lind et al. [10] reported that ferrochrome waste is less likely to distribute harmful heavy metals to the environment. Acharya and Patro [11] reported that ferrochrome waste can be used with lime instead of Portland cement in concrete production. In addition, it was stated that lime and ferrochrome waste added to the concrete mixture improved the flexural and compressive strength of the concrete. Panda et al. [12] used ferrochrome waste as aggregate in the production of portland cement and reported that they obtained high-strength concrete. Kumar et al. [13] explained that they produced concrete with high compressive strength with the ferrochrome waste they used as aggregate. In addition, there are studies in which higher compressive and flexural strength results of ferrochrome aggregate concrete are obtained compared to conventional aggregate concrete [2, 14]. Since there are not many studies on the mechanical properties of ferrochrome waste, it is necessary to determine the mechanical properties of concrete by optimizing the amount of ferrochrome waste in the concrete mixture, which is likely to be used instead of sand as an aggregate in concrete production. Furthermore, in experimental studies, it is expected that concrete's structural and mechanical properties will be improved with the components used as additives in cement mortar production. Compared to conventional concrete, conductive concrete is superior in terms of mechanical properties and cost, and concretes produced with additives used in conductive concrete mixture are used in application areas such as defrosting [15]. Studies are carried out to increase the mechanical properties of concrete with materials such as carbon nanotubes and carbon fiber (CF) included in cement-based mixtures [16]. It has been reported that CF concrete, which is one of the additives added to the concrete mix to give the concrete electrical properties, reduces the electrical resistance [17]. On the other hand, Chen and Liu [18] reported that the electrical resistance of the conductive concrete would increase in case of damage to the CF reinforced concrete. Roberts et al. [19] reported that CFs added to concrete improve the compressive and tensile strength of concrete. In addition, they explained that the damage to the conductive concrete can be determined by the relationship between the voltage applied to the concrete and its electrical resistance. Furthermore, CF incorporated into the concrete mix improves the mechanical properties of the concrete [20]. It has been confirmed by different studies that the electrical resistance of concrete is at high levels. While the electrical resistivity of outdoor dried concrete was determined as 6.54×10^5–11.4×10^5 Ω.cm, the electrical resistivity of saturated concrete and dry concrete were determined to be 10^6 Ω.cm and 10^9 Ω.cm, respectively [21]. There are various studies on the mechanical behavior of CF reinforced conductive concrete exposed to different loads such as pressure and bending [22]. In the literature, it has been reported that CF can inhibit microcrack growth in the study on the compressive strength of CF reinforced concrete [23]. Han et al. [24] stated that CF reinforced concrete has excellent compressive strength and high flexural strength compared to conventional concrete. Considering the use of industrial waste materials in concrete production and the studies on conductive concrete, research has been carried out to improve the strength properties of concrete by using recycled ferrochrome instead of aggregate. In addition, the CF additive in concrete was investigated in terms of both conductivity and mechanical properties. Studies on improving the mechanical properties of concrete by recycled ferrochrome, which is used as aggregate in concrete production, are limited. In addition, no studies have been conducted in which recycled ferrochrome and CF are used together in the concrete mix. In this paper, the effects of using recycled ferrochrome instead of aggregate used in the cement mixture and CF used as an additive on the microstructure, mechanical and electrical conductivity properties of the cement mortar were investigated. To understand the effect of recycled ferrochrome and CF on the performance of concrete, compressive strength, flexural strength, dynamic resonance, ultrasonic pulse velocity (UPV), Leeb hardness, and dry density tests were carried out. Considering that it will provide both low cost and energy savings, the use of recycled ferrochrome and CF mixture in the concrete mixture is research conducted to improve the mechanical and electrical properties of conductive concrete.

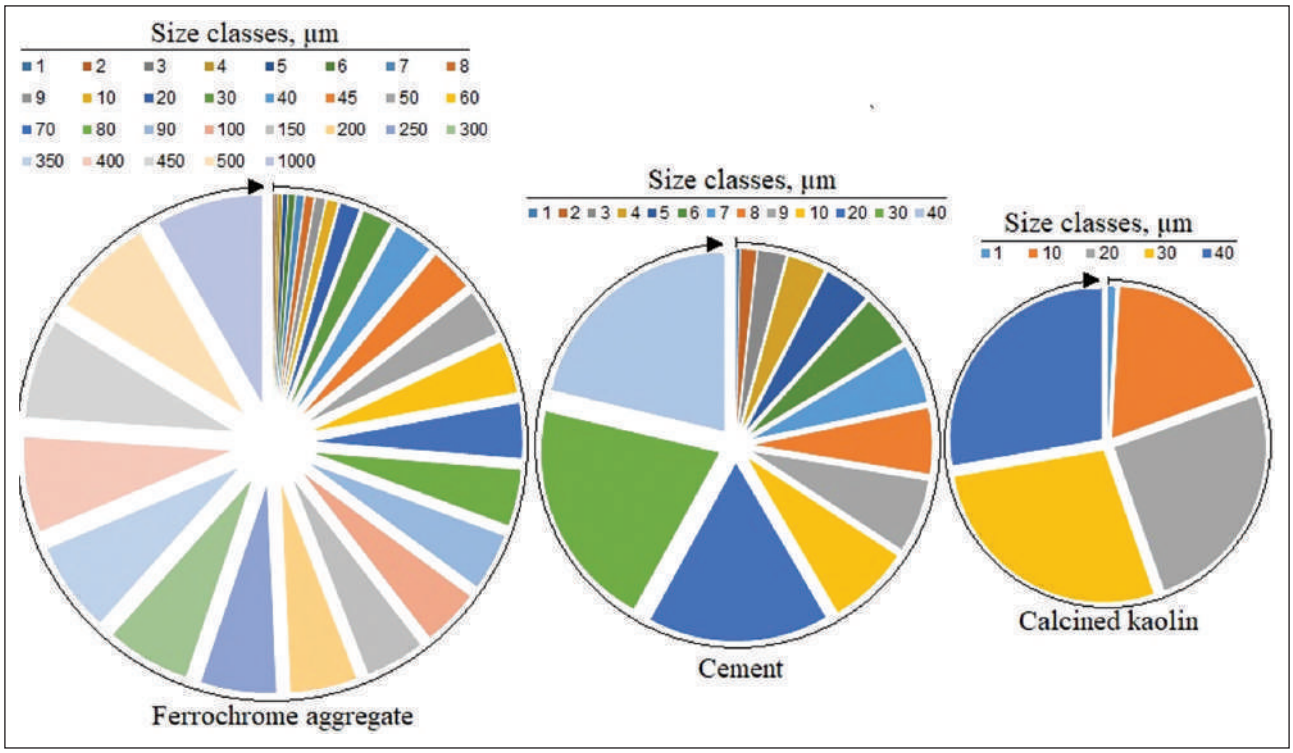

Figure 1. Grain size range of ferrochrome, cement, and calcined kaolin.

2. MATERIAL AND METHODS

2.1. Material Properties

100% ferrochrome aggregate was used as the filling material in all mixtures. The specific gravity of ferrochrome aggregate used was 3.33. CEM II-42.5 R white cement, preferred in facade cladding, was used as a binder. In all mixtures, 10% calcined kaolin by weight of cement was preferred. The particle size ranges of ferrochrome, cement, and calcined kaolin were compared in Figure 1. 12 mm long, 7.2 µm diameter, and 0.00155 Ω.cm electrical resistivity CF has been used as conductivity enhancing fiber. Carboxymethyl cellulose (0.2 wt%), which has been proven to have a positive effect in several previous studies [25–27], was used as a dispersing agent. Different ratios of polycarboxylate-based superplasticizers were used to ensure adequate workability in all mixtures.

The material content of the conductive mixtures produced within the scope of the study is summarized in Table 1. The mixture in the table's first row can be considered the matrix for all mixtures. All dry and liquid materials were weighed to form the matrix, and the dry materials were placed in the mixer for 90 seconds. 70% of the water was added and mixed for another 60 seconds. Finally, the required plasticizer was added to 30% of the water and added to the mixture, and the mixing process was continued for 60 seconds. After all the components came together in CF mixtures, when the matrix was ready, the fibers were added and mixed with a mixer for 90 seconds.

2.2. Test Methods

For all the planned tests, three 40x40x160 mm prismatic specimens were produced from each mixture, and all tests were performed on identical specimens, primarily non-destructive ones. The electrical resistivity of cementitious materials is measured for different purposes. For example, electrical resistivity values are measured, especially for corrosion detection in rebar reinforced structural elements. In these studies, the four-probe technique or other superficial test techniques are used as the measurement method. Since the resistivity measurement reason in the current study was to specify the bulk conductivity of the samples, the two-point uniaxial measurement method, which is also frequently used in the literature [21, 28], was preferred. A potential difference of 40 volts was applied to all samples for resistivity measurement. The frequency was kept constant at 50 Hz throughout the measurement. Longitudinal resonance frequency testing was performed for all mortar samples according to the ASTM C215 standard [29]. In this test method, the specimen is fixed midway between two supports, and a slight impact is applied from one end of the specimen, while the impact response from the other end is measured with an accelerometer. Resonance frequency diagrams are drawn for each sample using the data obtained with the accelerometer, and accordingly, the damping ratio of the mortars is determined.

Flexural and compressive strength tests were carried out following the TS EN 196-1 standard [30]. UPV tests were performed according to ASTM C597 [31]. The ASTM A956 standard [32] was used to determine the Leeb hardness of

Table 1. Component ratios in mixtures

No	Code	Ferrochrome slag aggregate (g)	Cement (g)	Calcined kaolin (g)	Water (g)	CF (g)	Superplasticizer (g)
1	Ref	1550	500	50	231	0.0	6.25
2	CF-0.50	1541	500	50	231	9.0	8.25
3	CF-0.75	1537	500	50	231	13.5	9.0
4	CF-1.0	1533	500	50	231	18.0	10.75

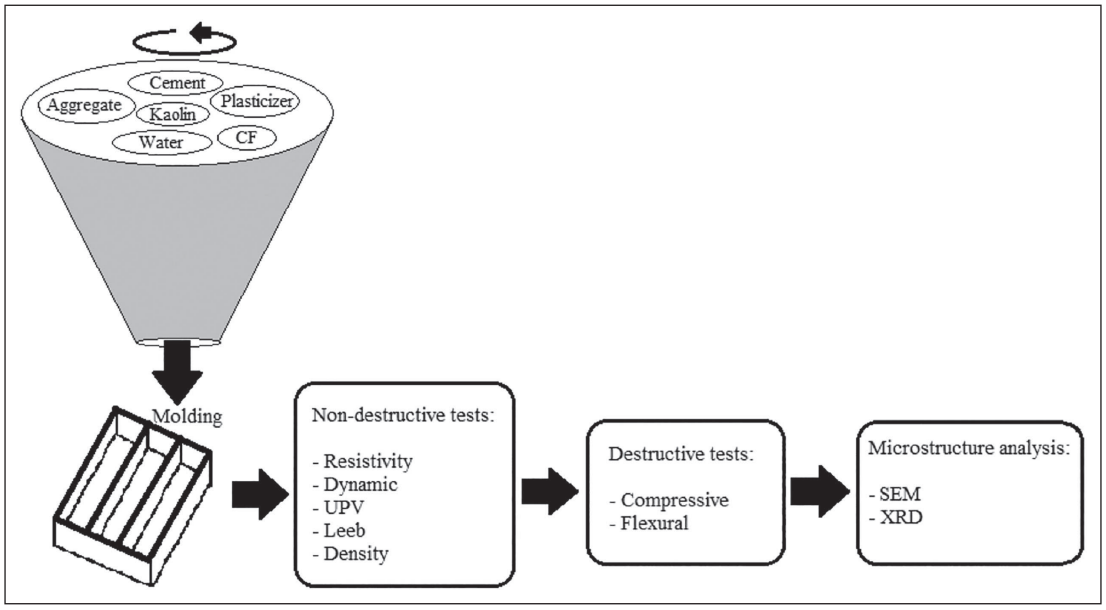

Figure 2. Experimental flow flowchart.

the produced samples. In addition, densities were calculated by measuring the dry weight and dimensions of all 28-day samples. The surface characterization of the mixture's ferrochrome aggregate used as aggregate was made by scanning electron microscopy (SEM) and elemental characterization by Energy Dispersive X-Ray Analysis (EDX). In addition, SEM and XRD analyses of FRC and FRC-0.75CF samples were performed. The experimental flow realized within the scope of the study is shown in Figure 2.

3. RESULTS AND DISCUSSION

3.1. Mechanical Test Results

The compressive and flexural strength test results of concrete samples are shown in Figure 3 comparatively. The CF additive component affected the mechanical properties of the conductive concrete. The compressive strength values of the samples vary between 66 MPa and 71 MPa. The highest compressive strength was determined in the 0.50 CF reinforced FRC-0.50CF sample. On the other hand, the compressive strength decreased with the increase of CF content in the cement mixture. Compared to the FRC-0.50CF sample, the compressive strength values in the FRC-0.75CF and FRC-1.0CF samples decreased by approximately 4% and 5%, respectively. It could be stated that the compressive strength value of the FRC-0.50CF sample is higher than the other samples, and the increased CF reinforcement element in the conductive concrete mixture causes a decrease in the compressive strength.

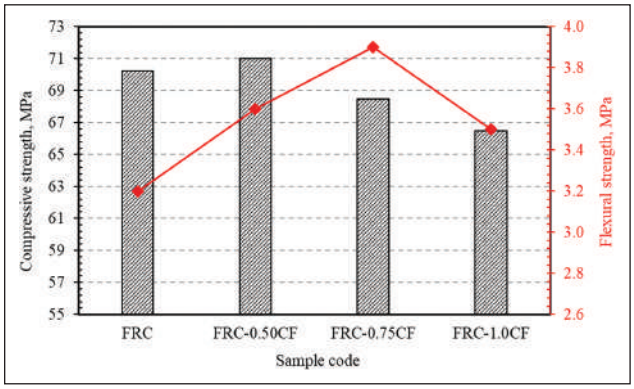

Figure 3. Compressive and flexural strength test results.

On the other hand, the flexural strength results of the samples are in the range of 63 to 72 MPa. The flexural strength test results increased with 0.50% CF added to the

concrete sample, as in the compressive strength test results. In the next test, the flexural strength value of the concrete of 0.75% CF reinforcement component in the cement mixture is 72 MPa. In the final test specimen, the flexural strength value decreased with increasing the CF content in the mixture to 1.0%. The flexural strength values of the FRC-0.50CF and FRC-1.0CF samples decreased approximately 5% and 8%, respectively, compared to the FRC-0.75CF sample with the highest flexural strength value. The flexural strength value of the ferrochrome-filled concrete sample without CF reinforcement is lower than that of the CF reinforced samples and could be associated with the improvement of the flexural strength of the concrete sample by the CF reinforcement component in the cement mixture. The flexural strength test results can be correlated with the load bearing capacity corresponding to the crack in the concrete material. Thus, the CF reinforcement increased the flexural strength by resisting crack propagation in the concrete material. Compressive strength in concrete materials containing CF reinforcement components was similar to flexural strength performance. While the highest compressive strength effect of the concrete material was achieved with 0.5% CF, the highest flexural strength increase was obtained with 0.75% CF. Al-Shamayleh et al. [33] associated the increase in compressive strength with high elasticity and reported that it contributed to the flexural strength. In addition, Chen et al. [23] pointed out that CF concrete increases compressive strength and prevents fractures in the concrete material. Therefore, it could be said that the ferrochrome-filled CF reinforced cement mixture provides compressive strength and flexural strength increase on the concrete material and prevents the spread of crack damage in the concrete structure.

3.2. Non-Destructive Test Results

3.2.1. Electrical Resistivity

Electrical resistivity values of 2, 14, 28, 90, and 180 days were measured and compared in Figure 4. Considering the time effect on the resistivity results, the resistivity values increased with the advancing age of the sample in all mixtures. This was more evident in the pure mixture without conductive fibers compared to the conductive mixtures. In FRC, FRC-CF0.5, FRC-CF0.75 and FRC-CF1.0 mixtures, 180-day resistivity values increased 6.07, 2.30, 1.16 and 1.23 times, respectively, compared to 2-day. This means that the conductivity of the materials decreases at these rates over time. When the resistivity values of 0.5%, 0.75%, and 1% CF added mixtures were compared with the pure sample, 56, 206, and 289 fold reductions were observed at 180-day values. The reason for the excessive conductivity loss of the pure mixture compared to the conductive mixtures is the presence of water in the matrix, the factor in which it conducts the current in this mixture. In cementitious materials, conductivity decreases with the evaporation of water

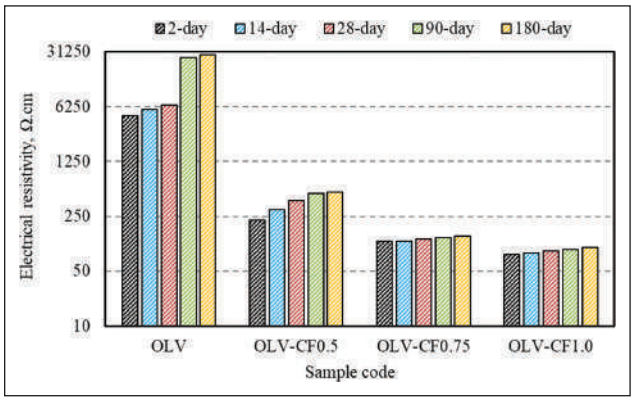

Figure 4. Electrical resistivity results from mortar specimens.

and the completion of hydration processes over time [34]. In conductive mortars, conductivity values were more stable since the current flow path was through the fibers. In the present study, 2-day resistivity values were obtained between 80–4762 and 180-day values between 100-28921 Ω.cm. Different studies have confirmed that the electrical resistance of concrete is at high levels.

While the electrical resistivity of outdoor dried concrete was determined as 6.54 X 10^5–11.4 X 10^5 Ω.cm, the electrical resistivity of saturated concrete and dry concrete were determined to be 10^6 Ω.cm and 10^9 Ω.cm, respectively [21]. The specification of a conductivity class for concretes may vary for different purposes. For example, in the study of Dehghanpour et al. [34], the maximum resistivity value of a heat-producing concrete is approximately 500 Ω.cm. This value may vary in self-perceiving concretes. D'Alessandro et al. [35] presented a systematic investigation of various procedures to fabricate self-sensing carbon-nanotube-containing cementitious materials. The dispersion quality, decomposition rate, and SEM images of nanotubes were investigated using the dispersion of nanotubes in water, chemical dispersants, and different mixing strategies. The resistivity values of different mixtures containing 0-1.6% multi-walled carbon nanotube (MWCNT) were obtained between about 10^3–10^7 Ω.cm according to different experimental procedures. According to the results of the study, it was found that the minimum MWCNT content was 1% by weight of cement in order to obtain self-sensing cementitious materials.

3.2.2. Dynamic Resonance Test Results

The defects of conventional concrete, such as low tensile strength, low ductility, and low damping, can be replaced and improved with additive phase materials. In addition to the mechanical, durability, and physical properties of cementitious materials, examining their dynamic behavior is important for the health of the building. Therefore, it is advantageous to investigate the effects of fibers and additives in cementitious materials on dynamic properties such as damping ratio. Different methods in materials can ob-

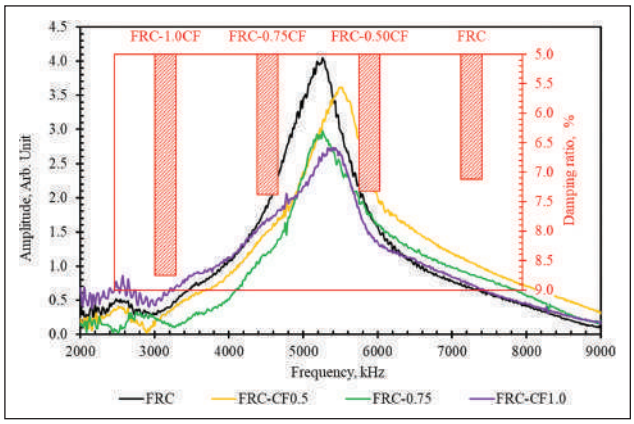

Figure 5. Damping ratio and amplitude-frequency curves.

tain the damping ratio. The half-Power method was used in this study. In the Half-Power method, the damping ratio is derived from the frequency spectrum of a structure's acceptance. For this, the upper and lower frequency values with an amplitude of 0.707 times the peak of the response signal are found. The damping ratio is calculated by dividing the difference between the upper and lower frequencies by twice the natural peak frequency. Amplitude-Frequency curves obtained by subjecting samples produced from four different mixtures to a dynamic resonance test and their damping ratios are summarized in Figure 5. When the curves in the Figure are considered, the amplitude values vary between 2.7-4 units. Also, the peaks were around 5500 kHz. When the damping ratios are considered, it is observed that the damping property increases with the addition of CF and the increase in its ratio. Damping ratios vary between 7.1% and 8.7%. The damping ratios of 0.5%, 0.75% and 1.0% CF added mixtures increased by 2.8%, 3.8% and 23% compared to the pure mixture. In a research paper [36], the damping ratios of conventional concrete samples filled with recycled aggregates at different rates were between 1 and 4. Nabavi et al. [37], polypropylene fibers and styrene butadiene rubber (latex) were selected for use in the concrete mix to obtain highly damped concrete. Four categories of laboratory concrete samples, including plain concrete, fiber reinforced concrete, polymer modified concrete, and fiber used in polymer modified concrete, were poured and tested to determine the damping rate of these concrete categories. Experiments have shown that polymer-concrete composites can absorb dynamic load energy much faster than conventional concrete. Therefore, the positive effects of synthetic fibers on the damping rate have been proven in the literature [38]. In Figure 5, when the curves and damping ratio results are compared, steeper peaks show lower damping and lower peak higher damping. This situation is explained in the literature as follows. It is known that narrow and steep Frequency-Amplitude curves have less damping properties of the relevant material, and wide and low curves have higher damping properties [39].

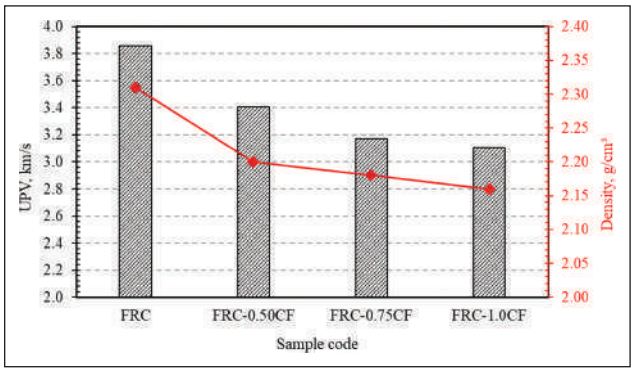

Figure 6. Ultrasonic pulse velocity test results.

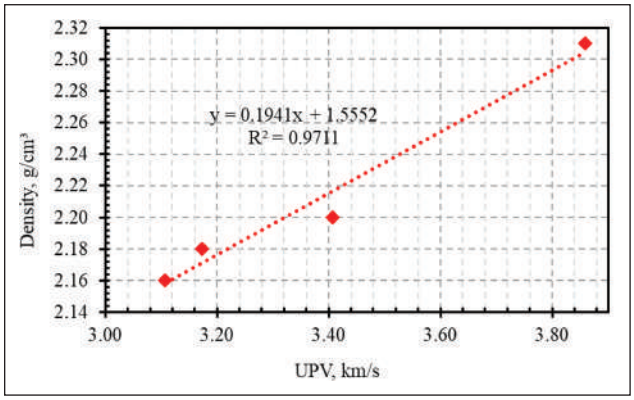

Figure 7. Relationship between UPV and density.

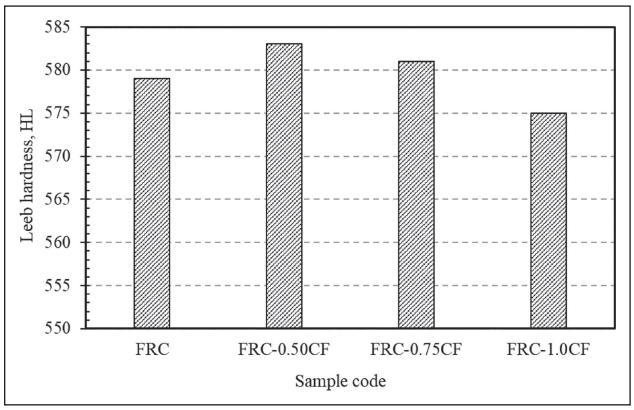

Figure 8. Leeb hardness test results.

3.2.3. Ultrasonic Pulse Velocity (UPV)

UPV and density measurement results of the prepared samples are shown in Figure 6. It is seen that the UPV and density values of the samples decrease with the CF additive added to the mixture. The highest UPV and density values are 3.9 km/s and 2.32 g/cm^3 in the FRC sample, respectively. Vilaplana et al. [40] reported that the UPV and density values of high-strength materials showed linear similarity with the compressive strength. Also, Dabbaghi et al. [41] reported that interparticle voids occur in fiber-containing

concrete samples. They also explained a direct relationship between UPV and concrete density. It can be said that adding CF to the ferrochrome-filled cement mixture harms the compact structure of the matrix by reducing the UPV and density values.

On the other hand, it could be concluded that CF reinforcement, which provides the increase in compressive strength and flexural strength, is not effective on these parameters. When the UPV and density test results in Figure 7 are compared with the compressive strength test results in Figure 3, it is seen that the UPV and density values of the FRC-0.75CF sample with the highest compressive strength decreased. Thus, it is verified that the compact structure in the concrete material is obtained by ferrochrome filling. As stated by Dawood et al. [42], adding fiber to the mixture increased the porosity formation by decreasing the workability of the mixture. The CF in the cement mixture reduced the UPV velocity wave throughout the sample, decreasing the UPV value.

3.2.4. Leeb Hardness Results

Figure 8 shows the Leeb hardness test results of the samples. It is seen that there is a compatibility between the pressure values mentioned above and the Leeb hardness results. It is observed that the Leeb hardness value of the concrete sample increased with 0.5% CF added to the ferrochrome-filled cement mixture. On the contrary, the Leeb hardness value decreased with increasing CF content in the mixture. Gomez-Heras et al. [43] reported that the Leeb hardness value is related to porosity. It could be stated that the ferrochrome filler in the mixture fills the porous structures of the concrete material and thus contributes to the increase in strength of the concrete. In addition, adding CF to the mixture improved the Leeb hardness of the sample. It could be said that the CFs in the FRC-0.5CF sample with the highest Leeb hardness are evenly distributed in the mixture, and sufficient fiber reinforcement is made. The decrease in Leeb hardness value with the increase of CF in the mixture can be attributed to the fact that CFs begin to cluster in the mixture and form porosity in the structure. There are a few Leeb hardness studies on regular concretes, although limited. Song et al. [44] investigated the Leeb hardness of sodium silicate-based concrete and regular C30 concrete and concluded that the average hardness value of regular concrete was 362 HL, and that of sodium silicate-based concrete was 405 HL. In [38] studies, Lebb hardness values for UHPCs were measured between 620-640 HL. Lebb hardness values measured for samples vary between 575-583 HL.

3.2.5. Microstructure Analysis Results

SEM analysis of the ferrochrome aggregate, whose pictures are shown at three different resolutions, is given in Figures 9 a, b, and c. SEM images provide information about the pore structure of ferrochrome. Angular irregular distribution of ferrochrome particles is observed. The roughness of the particle surface shown in Figure 9 b can be attributed to the ferrochrome aggregate's strong adhesion with the cement mix's components. The microstructure of the high-magnification ferrochrome in Figure 9 c has seen a dense layer form. The fact that there are almost no voids in the ferrochrome structure could be attributed to the fact that crack formation can be prevented. In addition, it could be stated that when used instead of aggregate in ferrochrome cement mixture, it can increase concrete quality and contribute to compressive strength. The EDS results from the analysis of the selected area in Figure 9 c are shown in Figure 9 d. The presence of aluminum (Al), silica (Si), iron (Fe), and chromium (Cr) in the structure of ferrochrome aggregate from EDS peaks was determined. Also, the chemical composition is given in the table in Figure 9 d. It is seen that ferrochrome aggregate contains 52.85% Cr, 39.68% Fe, 6.29% Si, and 1.18% Al by weight. The very low carbon content can explain the absence of the C peak in the EDS analysis of the product. However, low levels of Al and Si contents confirm the high purity ferrochrome aggregate. The presence of elements such as Al and Si other than Fe and Cr elements in the ferrochrome structure is explained by the different spinel structures of ferrochrome [45].

The XRD analysis of the ferrochrome aggregate is shown in Figure 10. Also, the crystal phases analyzed from the x-ray diffraction of ferrochrome in Figure 10 are shown in the table. It can be noted that the seven minerals detected are stable products and intensify the microstructure mentioned above. Also, it can be stated that the crystal phase minerals contribute to the increase in strength in the ferrochrome-filled concrete sample [46]. In addition, The broadening peak between 2θ: 10 and 20 can be explained by the presence of the amorphous phase [7]. It is observed that crystalline phases of minerals mainly containing chromium and iron are formed.

On the other hand, the crystal phase formation of quartz, calcite, magnesium, and aluminum minerals is low. It is seen that the most intense peaks are seen in the crystal phase structures of the chromferide and fayalite minerals. The formation of calcite and quartz crystal phases can be associated with the mentioned C-S-H (Calcium Silicate Hydrate) formation in the microstructure of ferrochrome. Islam et al. [47] reported that the mineralogical properties of ferrochrome are complex due to the presence of chromium in different oxide states. On the other hand, in the crystal phase analysis of the ferrochrome aggregate characterized in this study, it was observed that only the chromferide mineral contained Cr.

Figure 11 shows the ferrochrome-filled pure FRC sample's SEM images at different magnifications. The surface morphology of the FRC sample gives information about the pore structure and crack formation. The rough surface morphology seen in Figure 11 a can be associat-

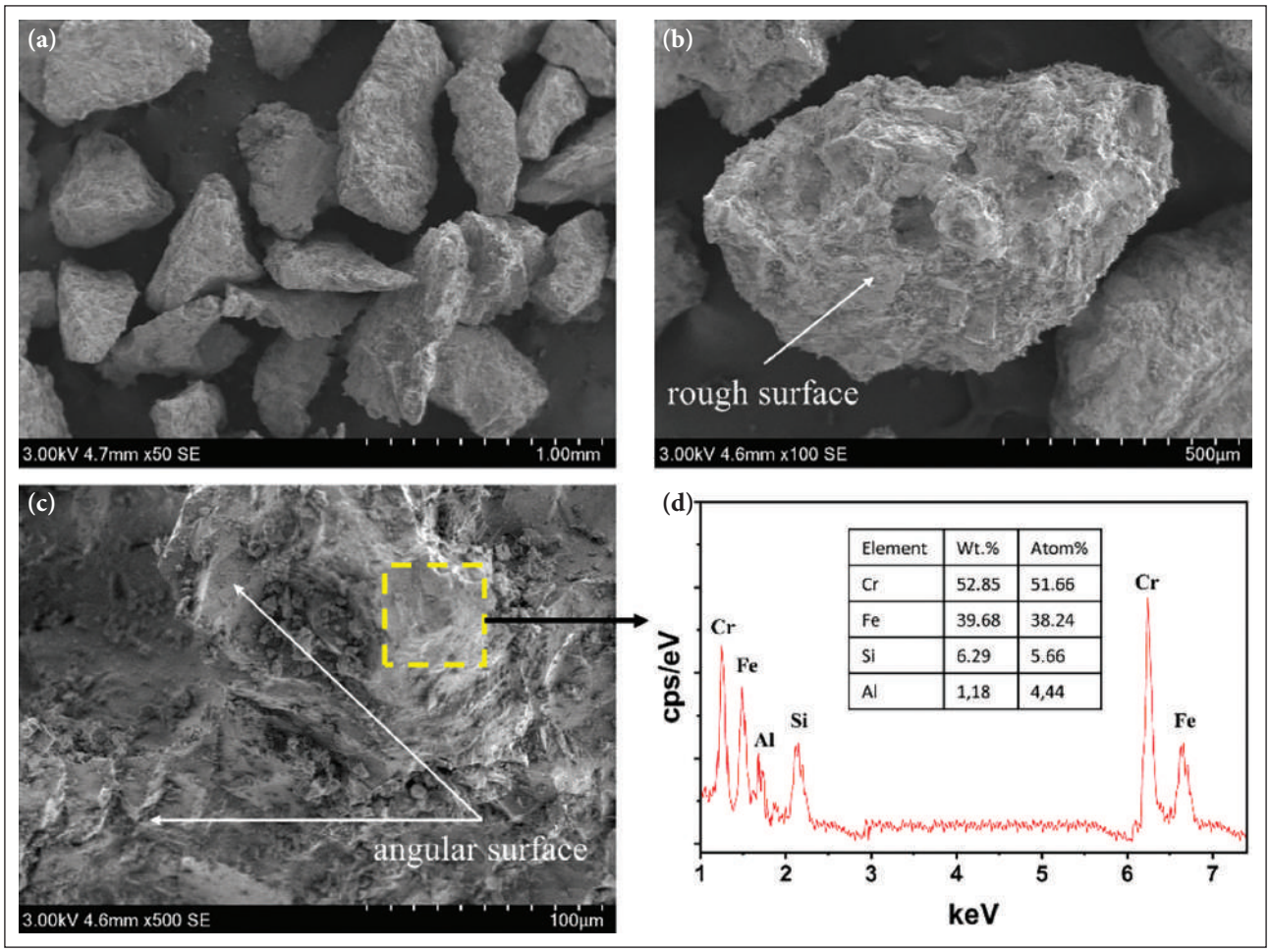

Figure 9. SEM images of ferrochrome aggregate **(a–c)**, EDS analysis of ferrochrome aggregate **(d)**.

ed with the rough surface of the ferrochrome mentioned above aggregate. In addition, the surface roughness of the ferrochrome aggregate significantly affected the bond strength in the cement mixture. However, at higher magnification microstructures (Fig. b and c), the aggregates appear to be irregularly dispersed angled particles. Moreover, the presence of C-S-H formations is related to the dense structure in the microstructure. The fact that the porous structure seen in Figure 11 c is not typical throughout the sample can be attributed to the inhibition of the increase in porosity by the dense structure of the ferrochrome aggregate.

The SEM image of the conductive concrete sample (FRC-0.75CF) in which CFs close to each other form a conductive network is given in Figure 12 a. Figure 12 b shows the high-magnification microphotograph of the SEM image with CF. SEM analyzes show that CF reinforcement reduces porosity in the microstructure. It could be stated that CFs in the cement matrix accelerate the formation of C-S-H, increasing the nucleation regions where stable growth occurs, filling the porous structure, and thus increasing the strength of the concrete sample [48]. In addition, it could

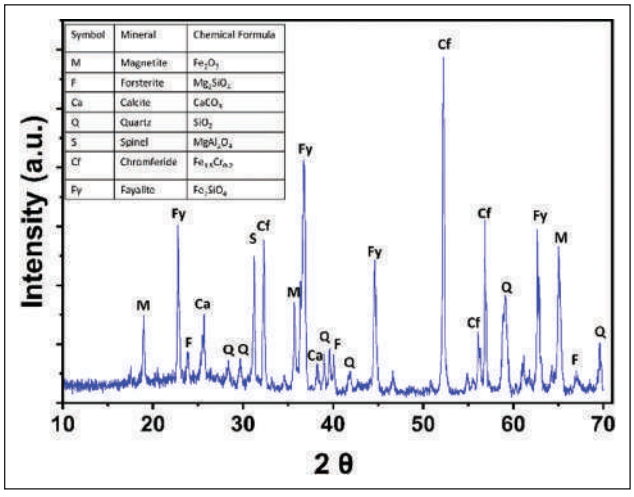

Figure 10. XRD patterns of ferrochrome aggregate.

be said that the fibers in the sample containing 0.75% CF do not agglomerate and do not adversely affect the strength properties mentioned above. Adding more than 0.75% CF to the cement mix causes the fibers to clump together,

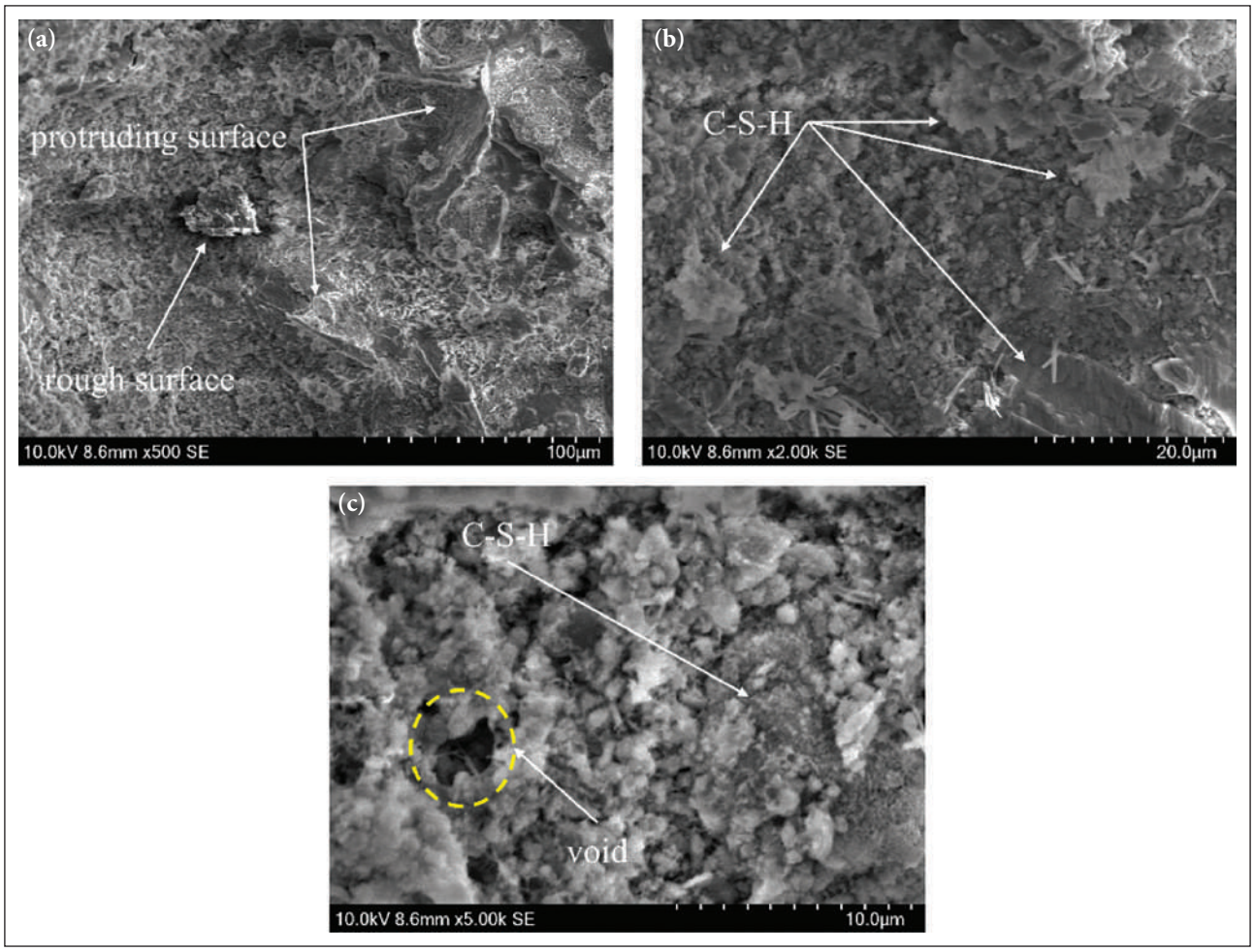

Figure 11. SEM microphotograph of FRC sample.

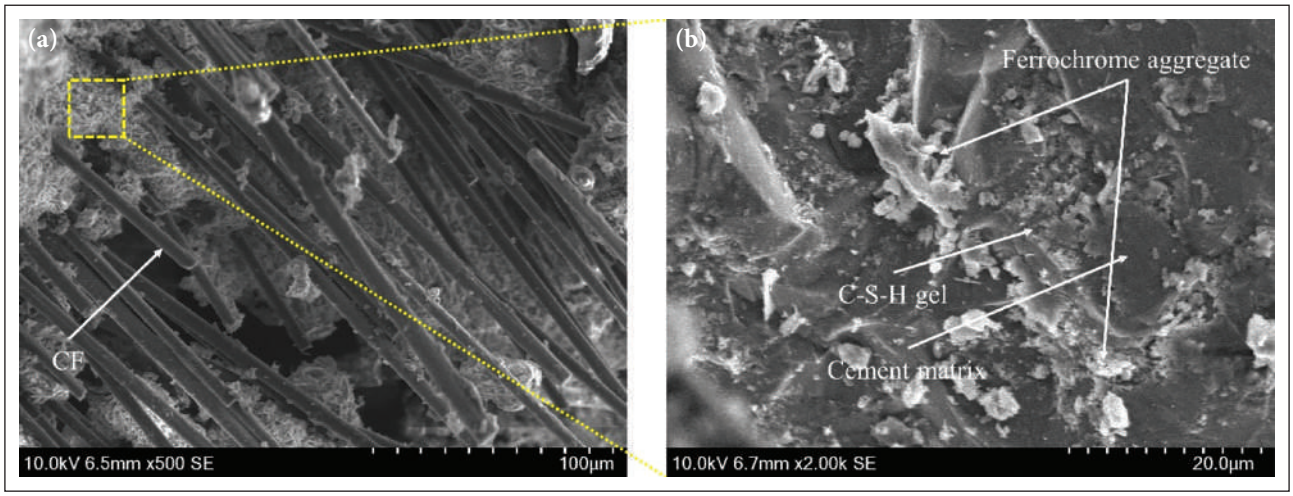

Figure 12. SEM images of conductive concrete FRC-0.75CF sample.

weakening the cement matrix, and crack propagation cannot be prevented. The compact microstructure formed by the ferrochrome aggregate particles settling in the cement matrix with CFs contributed to the increase mentioned above in compressive strength. Also, the increased compressive and flexural strength of the CF mentioned above added concrete sample could be correlated with the dense microstructure shown in Figure 12 b.

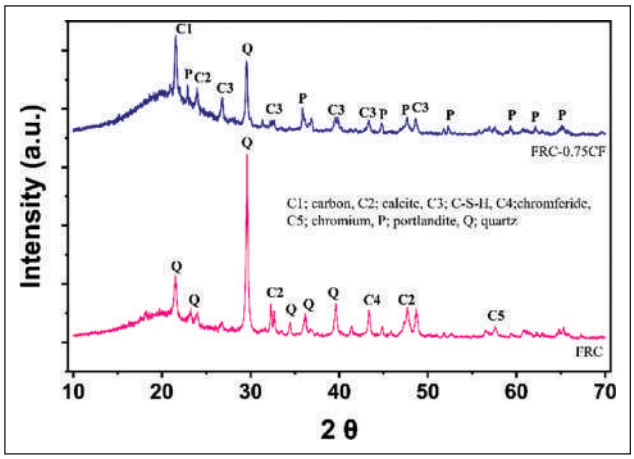

Figure 13. XRD patterns of ferrochrome filled (FRC) and carbon fiber reinforced cement (FRC-0.75CF).

Moreover, the increase in compressive strength in the 0.75% CF-added mortar sample was explained by the absence of ettringite formation, which causes internal stresses and cracks in the microstructure [49]. On the other hand, homogeneously distributed CFs formed a conductive network (Fig. 12 a). CF fibers in sample FRC-0.75CF increased the conductivity of the concrete by decreasing the electrical resistivity. The increase in conductivity can be explained by the CFs that form a conductive bridge between the aggregate and matrix in the cement mixture. It can be said that the cement hydration products seen in Figure 12 b adhere to the CF and increase the strength of the conductive concrete.

The crystal structures of the FRC and FRC-0.75CF samples and the minerals in the table are shown in Figure 13. In the XRD analysis of the FRC sample, the most quartz peaks are seen, and the chromeferide peak, which contains Cr and Fe elements in the ferrochrome aggregate structure, was found. Also, the chromium phase was formed although at low peak intensity. The quartz mineral with the highest peak intensity is explained by the availability of free silica [50]. Compared to the FRC-0.75CF sample, it is seen that the quartz peak density in the FRC sample is higher. In the XRD analysis of the ferrochrome mentioned above aggregate, the high densities of the mineral phases turned into low-intensity phases in the FRC sample. It can be attributed to the different reactions that take place in the cement mixture of the ferrochrome aggregate.

Moreover, compared to the FRC sample, the XRD analysis of the FRC-0.75CF sample shows carbon, portlandite, and C-S-H crystal phases. In the XRD patterns of the FRC-0.75CF sample, it is seen that the peak of the carbon crystal is intensity. Also, portlandite and C-S-H compositions contributed to the surface interaction between cement matrix and CF. The fact that the main crystalline phases are carbon and quartz can be attributed to the workability of the conductive network in the cement matrix [51]. The low peak densities of the C-S-H phases may be associated with the reaction in the cement mixture. In addition, C-S-H characterized at different diffraction angles can be attributed to the compactness of the microstructure and the increase in strength in the concrete sample. C-S-H phase formation, which is compatible with the SEM images of the FRC-0.75CF sample, contributed to the compressive strength of the concrete sample. Also, the increase in compressive strength can be attributed to the collapse of the C-S-H gel around the CFs. In addition, according to Bai et al. [52], the high carbon peak intensity was attributed to the high specific surface area of the carbon and its association with other particles. It has also been reported that carbon particles in the cement mixture improve the hydration reaction. However, it is stated that the small gaps between the carbon particles cause the gaps in the cement mixture to increase, thus reducing the compressive strength of the concrete [53, 54]. It can be said that the effect of CFs on the strength increase is limited despite the increased matrix strength in the ferrochrome-filled cement mixture.

4. CONCLUSIONS

In this article, the effects of ferrochrome filler used instead of aggregate and CF added to the cement mixture as reinforcement in different proportions on the compressive strength, flexural strength, UPV, density, electrical resistivity, and Leeb hardness of the concrete sample were investigated. In addition, the effect of CF on the microstructure and phase formations in the cement matrix in the FRC-0.75CF sample, which has optimum values in mechanical and conductivity test results, was characterized. According to the resistivity test results, the age effect of ferrochrome slag aggregate-filled conductive mortars was more evident in the first ages, and the age effect decreased over time. Almost no age effect was observed in CF-added mixtures. With the addition of CF, the resistivity values decreased approximately 40 times compared to the reference. The lowest resistivity value was measured for the mixture containing 1% CF. According to the damping ratio values obtained from the dynamic resonance test results, adding CF improved the damping property, and the maximum increase was calculated for the mixture containing 1% CF as 23%.

CF's compressive and flexural strength effects on concrete materials were similar. In the above-mentioned compressive strength test results, the FRC-0.75CF sample with the highest value provided 2 MPa higher compressive strength than the unreinforced FRC sample. Also, among the CF reinforced samples, the compressive strength of the FRC-0.75CF sample was 5 MPa higher than that of the FRC-1.0CF sample. In the flexural strength test results, the use of CF in the cement mixture positively affected the concrete's mechanical properties. FRC-0.75CF sample with the highest flexural strength value has 9 MPa and 6 MPa more strength compared to unreinforced FRC and reinforced FRC-1.0CF samples, respectively.

On the contrary, increasing the CF content added to the mix did not improve the UPV and density results. While adding CF decreased the UPV value to 3.1 km/s, the increase in compressive strength confirmed the relationship between the ferrochrome filler in the mixture and the UPV. Ferrochrome filler reduced the porosity and increased the UPV value of the hardening concrete. UPV and density measurement results showed that the FRC-filled plain concrete sample had a compact structure with less damage than the CF-added concrete samples. Leeb hardness test results, which show parallelism with the compressive strength values, confirmed the effect of filler and additive material. While the ferrochrome filling in the mixture increased the density of the structure, the CF reinforcement increased the strength of the concrete sample up to a certain extent. In the SEM analysis of ferrochrome aggregate, almost no void structure and hydration product formation were observed. SEM analysis results contributed to the reduction of porosity in the matrix by densifying the cement matrix of 0.75% CF. In addition, C-S-H formations in the microstructure improved the compact structure, and the absence of ettringite structures facilitated increased mechanical strength. Moreover, SEM analyses of the FRC-0.75CF sample showed that the CFs adhered to form a conductive network between the components in the ferrochrome-filled compact structure.

As a result, ferrochrome-filled CF reinforced concrete, which is recommended instead of regular concrete, which is widely used in the construction industry, offers superior mechanical and electrical properties compared to regular concrete by providing low production cost and energy savings in production.

DATA AVAILABILITY STATEMENT

The authors confirm that the data that supports the findings of this study are available within the article. Raw data that support the finding of this study are available from the corresponding author, upon reasonable request.

CONFLICT OF INTEREST

The authors declare that they have no conflict of interest.

FINANCIAL DISCLOSURE

This study was carried out within the scope of the project coded STB-072161 of Fibrobeton R&D Center. Thank you to Fibrobeton Company for their support. We also thank Eti Krom Inc. for their support of ferrochrome slag materials.

PEER-REVIEW

Externally peer-reviewed.

REFERENCES

[1] Islam, M. Z., Sohel, K. M. A., Al-Jabri, K., & Al Harthy, A. (2021). Properties of concrete with ferrochrome slag as a fine aggregate at elevated temperatures. *Case Studies in Construction Materials*, 15, e00599. [CrossRef]

[2] Al-Jabri, K., & Shoukry, H. (2018). Influence of nano metakaolin on thermo-physical, mechanical and microstructural properties of high-volume ferrochrome slag mortar. *Construction and Building Materials*, 177, 210–221. [CrossRef]

[3] Acharya, P. K., & Patro, S. K. (2016). Utilization of ferrochrome wastes such as ferrochrome ash and ferrochrome slag in concrete manufacturing. *Waste Management and Research*, 34(8), 764–774. [CrossRef]

[4] Abbass, W., Khan, M. I., & Mourad, S. (2018). Evaluation of mechanical properties of steel fiber reinforced concrete with different strengths of concrete. *Construction and Building Materials*, 168, 556–569. [CrossRef]

[5] de Alencar Monteiro, V. M., Lima, L. R., & de Andrade Silva, F. (2018). On the mechanical behavior of polypropylene, steel and hybrid fiber reinforced self-consolidating concrete. *Construction and Building Materials*, 188, 280–291. [CrossRef]

[6] Fares, A. I., Sohel, K. M. A., & Al-mamun, A. (2021). Characteristics of ferrochrome slag aggregate and its uses as a green material in concrete – A review. *Construction and Building Materials*, 294, Article 123552. [CrossRef]

[7] Al-Jabri, K., Shoukry, H., Khalil, I. S., Nasir, S., & Hassan, H. F. (2018). Reuse of Waste Ferrochrome Slag in the Production of Mortar with Improved Thermal and Mechanical Performance. *Journal of Materials in Civil Engineering*, 30(8), Article 0002345. [CrossRef]

[8] Dash, M. K., & Patro, S. K. (2018). Effects of water cooled ferrochrome slag as fine aggregate on the properties of concrete. Construction and Building Materials, 177, 457–466. [CrossRef]

[9] Niemelä, P., & Kauppi, M. (2007). Production, characteristics and use of ferrochromium slags. *Innovations In The Ferro Alloy Industry - Proceedings of the XI International Conference on Innovations in the Ferro Alloy Industry, Infacon XI*, 171–179.

[10] Lind, B. B., Fällman, A.-M., & Larsson, L. B. (2001). Environmental impact of ferrochrome slag in road construction. *Waste Management*, 21(3), 255–264. [CrossRef]

[11] Acharya, P. K., & Patro, S. K. (2015). Effect of lime and ferrochrome ash (FA) as partial replacement of cement on strength, ultrasonic pulse velocity and permeability of concrete. *Construction and Building Materials*, 94, 448–457. [CrossRef]

[12] Panda, C. R., Mishra, K. K., Panda, K. C., Nayak, B. D., & Nayak, B. B. (2013). Environmental and technical assessment of ferrochrome slag as concrete aggregate material. *Construction and Building Materials*, 49, 262–271. [CrossRef]

[13] Kumar, B. A. V. R., Keshav, L., Sivanantham, P. A., Arokiaraj, G. G. V., Rahman, D. R. Z., Kumar, P. M., & Somashekar, D. (2022). Comprehensive characterization of ferrochrome slag and ferrochrome ash as sustainable materials in construction. *Journal of Nanomaterials*, 2022, Article 8571055. [CrossRef]

[14] Acharya, P. K., & Patro, S. K. (2018). Bond, permeability, and acid resistance characteristics of ferrochrome waste concrete. *ACI Materials Journal*, 115(3), 359–368. [CrossRef]

[15] Kim, G. M., Yang, B. J., Ryu, G. U., & Lee, H. K. (2016). The electrically conductive carbon nanotube (CNT)/cement composites for accelerated curing and thermal cracking reduction. *Composite Structures*, 158, 20–29. [CrossRef]

[16] Mokhtar, M. M., Abo-El-Enein, S. A., Hassaan, M. Y., Morsy, M. S., & Khalil, M. H. (2017). Mechanical performance, pore structure and micro-structural characteristics of graphene oxide nano platelets reinforced cement. *Construction and Building Materials*, 138, 333–339. [CrossRef]

[17] Chiarello, M., & Zinno, R. (2005). Electrical conductivity of self-monitoring CFRC. *Cement and Concrete Composites*, 27(4), 463–469. [CrossRef]

[18] Chen, B., & Liu, J. (2008). Damage in carbon fiber-reinforced concrete, monitored by both electrical resistance measurement and acoustic emission analysis. *Construction and Building Materials*, 22(11), 2196–2201. [CrossRef]

[19] Roberts, R. H., & Mo, Y.-L. (2016). Development of carbon nanofiber aggregate for concrete strain monitoring. *In Innovative Developments of Advanced Multifunctional Nanocomposites in Civil and Structural Engineering* (pp. 9–45). Elsevier. [CrossRef]

[20] Hou, Z., Li, Z., & Wang, J. (2007). Electrical conductivity of the carbon fiber conductive concrete. *Journal Wuhan University of Technology, Materials Science Edition*, 22(2), 346–349. [CrossRef]

[21] Dehghanpour, H., & Yilmaz, K. (2020). Heat behavior of electrically conductive concretes with and without rebar reinforcement. *Medziagotyra*, 26(4), 471–476. [CrossRef]

[22] Vaidya, S., & Allouche, E. N. (2011). Strain sensing of carbon fiber reinforced geopolymer concrete. *Materials and Structures*, 44(8), 1467–1475. [CrossRef]

[23] Chen, M., Gao, P., Geng, F., Zhang, L., & Liu, H. (2017). Mechanical and smart properties of carbon fiber and graphite conductive concrete for internal damage monitoring of structure. *Construction and Building Materials*, 142, 320–327. [CrossRef]

[24] Han, J., Wang, D., & Zhang, P. (2020). Effect of nano and micro conductive materials on conductive properties of carbon fiber reinforced concrete. *Nanotechnology Reviews*, 9(1), 445–454. [CrossRef]

[25] Dehghanpour, H., Yilmaz, K., Afshari, F., & Ipek, M. (2020). Electrically conductive concrete: A laboratory-based investigation and numerical analysis approach. *Construction and Building Materials*, 260, Article 119948. [CrossRef]

[26] Dehghanpour, H., & Yilmaz, K. (2020). Investigation of specimen size, geometry and temperature effects on resistivity of electrically conductive concretes. *Construction and Building Materials*, 250, Article118864. [CrossRef]

[27] Dehghanpour, H., & Yilmaz, K. (2021). A more sustainable approach for producing less expensive electrically conductive concrete mixtures: Experimental and FE study. *Cold Regions Science and Technology*, 184, Article103231. [CrossRef]

[28] El-Dieb, A. S., El-Ghareeb, M. A., Abdel-Rahman, M. A. H., & Nasr, E. S. A. (2018). Multifunctional electrically conductive concrete using different fillers. *Journal of Building Engineering*, 15, 61–69. [CrossRef]

[29] ASTM C215. (2019). *Standard test method for fundamental transverse, longitudinal, and torsional resonant frequencies of concrete specimens*. American Society for Testing and Materials.

[30] TS EN 196-1. (2005). *Methods of testing cement–Part 1: Determination of strength*. Turkish Standard.

[31] ASTM C597. (2009). *Standard test method for pulse velocity through concrete*. American Society for Testing and Materials.

[32] ASTM A956. (2006). *Standard test method for leeb hardness testing of steel products*. American Society for Testing and Materials.

[33] Al-Shamayleh, R., Al-Saoud, H., Abdel-Jaber, M., & Alqam, M. (2022). Shear and flexural strengthening of reinforced concrete beams with variable compressive strength values using externally bonded carbon fiber plates. *Results in Engineering*, 14, Article 100427. [CrossRef]

[34] Dehghanpour, H., Yilmaz, K., & Ipek, M. (2019). Evaluation of recycled nano carbon black and waste erosion wires in electrically conductive concretes. *Construction and Building Materials*, 221, 109–121. [CrossRef]

[35] D'Alessandro, A., Rallini, M., Ubertini, F., Materazzi, A. L., & Kenny, J. M. (2016). Investigations on scalable fabrication procedures for self-sensing carbon nanotube cement-matrix composites for SHM applications. *Cement and Concrete Composites*, 65, 200–213. [CrossRef]

[36] Liang, C., Liu, T., Xiao, J., Zou, D., & Yang, Q. (2016). The damping property of recycled aggregate concrete. *Construction and Building Materials*, 102, 834–842. [CrossRef]

[37] Nabavi, F., Bhattacharjee, B., & Madan, A. (2011).

Improving the damping properties of concrete. *21st Australasian Conference on the Mechanics of Structures and Materials*, 867–872. [CrossRef]

[38] Dehghanpour, H., Subasi, S., Guntepe, S., Emiroglu, M., & Marasli, M. (2022). Investigation of fracture mechanics, physical and dynamic properties of UHPCs containing PVA, glass and steel fibers. *Construction and Building Materials*, 328, Article 127079. [CrossRef]

[39] Tian, J., Fan, C., Zhang, T., & Zhou, Y. (2019). Rock breaking mechanism in percussive drilling with the effect of high-frequency torsional vibration. *Energy Sources, Part A: Recovery, Utilization and Environmental Effects*, 44(1), 2520–2534. [CrossRef]

[40] Vilaplana, J. L., Baeza, F. J., Galao, O., Alcocel, E. G., Zornoza, E., & Garcés, P. (2016). Mechanical properties of alkali activated blast furnace slag pastes reinforced with carbon fibers. *Construction and Building Materials*, 116, 63–71. [CrossRef]

[41] Dabbaghi, F., Sadeghi-Nik, A., Libre, N. A., & Nasrollahpour, S. (2021). Characterizing fiber reinforced concrete incorporating zeolite and metakaolin as natural pozzolans. *Structures*, 34, 2617–2627. [CrossRef]

[42] Dawood, E. T., Mohammad, Y. Z., Abbas, W. A., & Mannan, M. A. (2018). Toughness, elasticity and physical properties for the evaluation of foamed concrete reinforced with hybrid fibers. *Heliyon*, 4(12), e01103. [CrossRef]

[43] Gomez-Heras, M., Benavente, D., Pla, C., Martinez-Martinez, J., Fort, R., & Brotons, V. (2020). Ultrasonic pulse velocity as a way of improving uniaxial compressive strength estimations from Leeb hardness measurements. *Construction and Building Materials*, 261, Article119996. [CrossRef]

[44] Song, Z., Xue, X., Li, Y., Yang, J., He, Z., Shen, S., Jiang, L., Zhang, W., Xu, L., Zhang, H., Qu, J., Ji, W., Zhang, T., Huo, L., Wang, B., Lin, X., & Zhang, N. (2016). Experimental exploration of the waterproofing mechanism of inorganic sodium silicate-based concrete sealers. *Construction and Building Materials*, 104, 276–283. [CrossRef]

[45] Mahamaya, M., & Das, S. K. (2020). Characterization of ferrochrome slag as a controlled low-strength structural fill material. *International Journal of Geotechnical Engineering*, 14(3), 312–321. [CrossRef]

[46] Dash, M. K., Patro, S. K., Acharya, P. K., & Dash, M. (2022). Impact of elevated temperature on strength and micro-structural properties of concrete containing water-cooled ferrochrome slag as fine aggregate. *Construction and Building Materials*, 323, Article 126542. [CrossRef]

[47] Islam, M. Z., Sohel, K. M. A., Al-Jabri, K., & Al Harthy, A. (2021). Properties of concrete with ferrochrome slag as a fine aggregate at elevated temperatures. *Case Studies in Construction Materials*, 15, e00599. [CrossRef]

[48] Barbhuiya, S., & Chow, P. (2017). Nanoscaled mechanical properties of cement composites reinforced with carbon nanofibers. *Materials*, 10(6), 662. [CrossRef]

[49] Nguyen, H.-A., Chang, T.-P., Shih, J.-Y., Chen, C.-T., & Nguyen, T.-D. (2016). Sulfate resistance of low energy SFC no-cement mortar. *Construction and Building Materials*, 102, 239–243. [CrossRef]

[50] Jena, S., & Panigrahi, R. (2019). Performance assessment of geopolymer concrete with partial replacement of ferrochrome slag as coarse aggregate. *Construction and Building Materials*, 220, 525–537. [CrossRef]

[51] Li, W., Pei, C., Zhu, Y., & Zhu, J.-H. (2021). Effect of chopped carbon fiber on interfacial behaviors of IC-CP-SS system. *Construction and Building Materials*, Article 275, 122117. [CrossRef]

[52] Bai, Y., Xie, B., Li, H., Tian, R., & Zhang, Q. (2022). Mechanical properties and electromagnetic absorption characteristics of foam Cement-based absorbing materials. *Construction and Building Materials*, 330, Article 127221. [CrossRef]

[53] Nambiar, E. K. K., & Ramamurthy, K. (2007). Air-void characterisation of foam concrete. *Cement and Concrete Research*, 37(2), 221–230. [CrossRef]

[54] Dehghanpour, H., Doğan, F., & Yılmaz, K. (2022). Development of CNT–CF–Al2O3-CMC gel-based cementitious repair composite. *Journal of Building Engineering*, 45, Article103474. [CrossRef]